Asian Journal of Mechanical Engineering
ISSN: 2249-6289 (P); 3049-1886 (E)
Vol.14 No.1, 2025, pp.39-50

www.crijournals.org
DOI: https://doi.org/10.70112/arme-2025.14.1.4287

Comparative Performance Analysis of Cu and Fe_3O_4 Nanofluids in Heat Transfer Applications

M. S. Sunitha[1], S. Kemparaju[2], R. D. Jagadeesha[3] and P. B. Sampath Kumar[4*]
[1]Department of Mathematics, Government First Grade College, Tumkur, Karnataka, India
[2]Department of Mathematics, Government First Grade College, Ramanagara, Karnataka, India
[3]Department of Mathematics, Government First Grade College for Women, Holenarasipura, Karnataka, India
[*4]Department of Studies and Research in Mathematics, Ramanagara PG Centre, Bangalore University, Karnataka India
E-mail: ms.sunitha0204@gmail.com, skemparaju74@gmail.com, jagadeesh25docs@gmail.com
*Corresponding Author: sampathkumarpb123@gmail.com
(Received 27 February 2025; Revised 25 March 2025; Accepted 15 April 2025; Available online 17 April 2025)

Abstract **- This study presents a comparative analysis of the heat transfer characteristics of copper (Cu) and magnetite (Fe_3O_4) nanofluids in a water-based medium. The three-dimensional flow of these nanofluids over a stretching surface is analyzed by incorporating the effects of Coriolis and Lorentz forces. The investigation further considers thermal radiation, viscous dissipation, Joule heating, internal heat generation, and convective boundary conditions to evaluate the efficiency of both nanofluids under identical operating conditions. The governing equations are formulated, reduced to a system of ordinary differential equations (ODEs) through similarity transformations, and solved numerically using the Runge-Kutta-Fehlberg (RKF) method. The results reveal that the Cu-based nanofluid exhibits superior heat transfer enhancement compared to the Fe_3O_4 nanofluid. These findings advance the understanding of nanofluid thermal performance in complex flow environments and provide insights for optimizing heat transfer efficiency in industrial and engineering applications.**

Keywords: **Nanofluids, Heat Transfer, Stretching Surface, Coriolis and Lorentz Forces, Runge-Kutta-Fehlberg (RKF) Method**

I. INTRODUCTION

The incorporation of nanoparticles into conventional base fluids has revolutionized the field of heat and mass transfer, giving rise to a new class of fluids termed nanofluids. Initially conceptualized by Choi and Eastman [1], nanofluids exhibit significantly enhanced thermal conductivity, viscosity control, and energy transport characteristics compared to traditional coolants. Due to their superior heat dissipation capabilities, nanofluids are extensively employed in high-efficiency cooling systems, micro-electromechanical systems (MEMS), nuclear reactors, and solar collectors [2]-[4].

Buongiorno [5] proposed a model accounting for seven slip mechanisms, including Brownian diffusion and thermophoresis, to explain the relative motion between nanoparticles and the base fluid. This formulation laid the foundation for accurate modeling of convective transport in nanofluids. Since then, numerous studies have extended the analysis to hybrid nanofluids, which incorporate multiple types of nanoparticles to optimize thermal performance. For instance, Muqaddass *et al.,* [6] investigated Cu-Al_2O_3-H_2O hybrid nanofluid behavior under convective boundary conditions and variable thermal conductivity. Similarly, Asadi *et al.,* [7] experimentally analyzed the rheological and thermal characteristics of CuO-TiO_2-H_2O hybrids, with emphasis on stability and viscosity behavior.

The heat and flow characteristics of nanofluids have also been explored under various external influences. Khan and Pop [8] examined boundary layer flow over stretching surfaces, relevant to polymer extrusion and thermal rolling. Sheikholeslami and Rokni [9] studied magnetohydrodynamic (MHD) effects on nanofluids under applied magnetic fields, while Nadeem *et al.,* [10] and Krishnamurthy *et al.,* [11] extended the investigation to non-Newtonian nanofluid flow and radiative heat transfer over exponentially stretching surfaces. Thus, numerous investigations on nanofluid dynamics have been reported by various researchers [12]-[20].

The role of rotational effects in fluid flow has emerged as a critical area of research due to applications in astrophysical flows, turbines, disk drives, viscometers, and centrifugal processing systems. The pioneering work of von Kármán [21] introduced similarity solutions for flow over a rotating disk, which was later extended by Wang [22] and Nazar *et al.,* [23] to account for unsteady and nonlinear effects. More recently, Makinde *et al.,* [24] analyzed nanofluid flow between rotating concentric cylinders within a porous medium, incorporating the influence of radial magnetic fields.

Rotational forces such as the Coriolis force (due to system rotation) and Lorentz force (due to magnetic field interactions) can significantly alter flow stability and thermal transport. Mustafa *et al.,* [25] studied nanofluid flow over a deformable surface subjected to Coriolis effects and nonlinear radiative flux. Archana *et al.,* [26] examined Casson nanofluids under MHD and thermal radiation conditions, considering Joule heating and viscous dissipation. Recently, Sampath *et al.,* [27] presented a detailed analysis of ferrofluid flow in a rotating system over

a deformed surface, incorporating Coriolis and Lorentz forces to evaluate their combined effects on energy transport.

Thermal radiation also plays a critical role in nanofluid performance, particularly in solar and high-temperature applications. Nanomaterials with tailored radiation absorption characteristics are increasingly utilized in photovoltaic and solar thermal systems. Hayat *et al.,* [28] investigated MHD stagnation-point flow over a porous medium with thermal radiation, while Motsumi and Makinde [29] analyzed nanofluid boundary layers under the combined influence of radiation and viscous dissipation. Other contributions, including those by Sheikholeslami *et al.,* [30], Reddy *et al.,* [31], and Waqas *et al.,* [32], emphasized nonlinear radiative effects in the presence of MHD, hybrid nanoparticles, and variable heat source/sink models.

Given these insights, the present study investigates the three-dimensional boundary layer flow of nanofluids over an expanding surface, incorporating copper (Cu) and magnetite (Fe_3O_4) nanoparticles. The model accounts for Coriolis and Lorentz forces, nonlinear thermal radiation, heat generation, viscous dissipation, Joule heating, and convective boundary conditions. The nonlinear governing equations are transformed using similarity variables and solved numerically via the Runge-Kutta-Fehlberg (RKF) method. The results of this study are expected to provide valuable insights for improving heat transport efficiency in rotating and thermally active industrial systems.

A. Mathematical Formulation

This study explores the three-dimensional rotational flow of electrically conducting nanofluids copper (Cu) and magnetite (Fe_3O_4) over a convectively heated stretching sheet in a water-based medium. The sheet is subjected to equal and opposite forces along the x-axis, resulting in a stretching velocity of $u_w = ax$, while the origin remains fixed. The nanofluid rotates uniformly around the z-axis with a constant angular velocity ω, and a uniform magnetic field B_0 is applied perpendicular to the flow direction. A convective heat transfer condition is imposed at the surface, where the temperature is maintained at T_f while the ambient temperature far from the surface is denoted as T_∞ representing the region beyond the thermal boundary layer (see Figure 1).

Following the famous Tiwari and Das model [33], the equations embodying the conservation of mass, momentum and energy are as follows;

$$\frac{\partial u}{\partial x}+\frac{\partial v}{\partial y}+\frac{\partial w}{\partial z}=0, \tag{1}$$

$$\rho_{nf}\left(u\frac{\partial u}{\partial x}+v\frac{\partial u}{\partial y}+w\frac{\partial u}{\partial z}-2\omega v\right)=\mu_{nf}\left(\frac{\partial^2 u}{\partial z^2}\right)-\sigma_{nf}B_0^2 u, \tag{2}$$

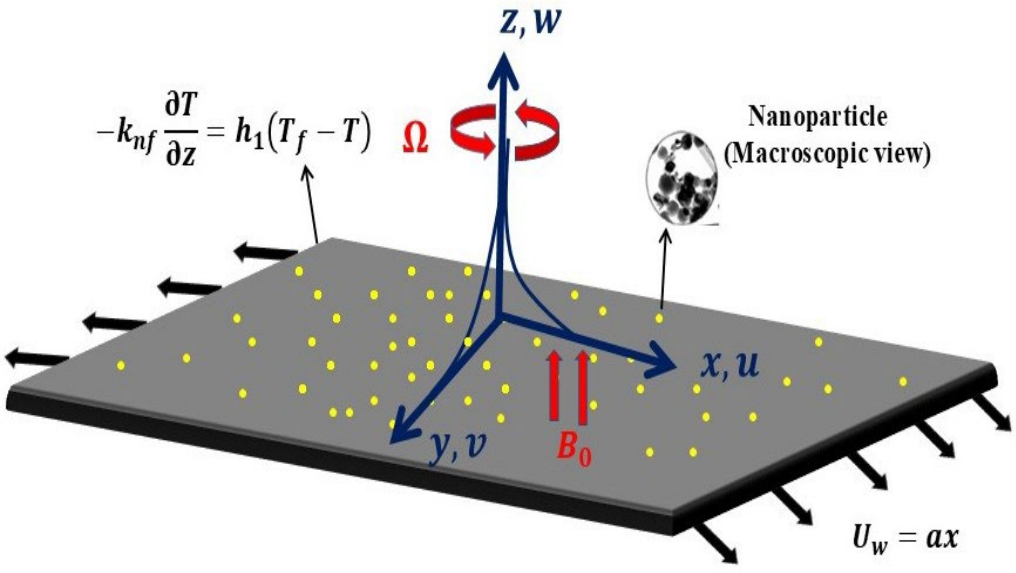

Fig.1 Geometry Of the Problem and Coordinate System.

$$\rho_{nf}\left(u\frac{\partial v}{\partial x}+v\frac{\partial v}{\partial y}+w\frac{\partial v}{\partial z}+2\omega u\right)=\mu_{nf}\left(\frac{\partial^2 v}{\partial z^2}\right)-\sigma_{nf}B_0^2 v, \tag{3}$$

$$u\frac{\partial T}{\partial x}+v\frac{\partial T}{\partial y}+w\frac{\partial T}{\partial z}=\alpha_{nf}\left(\frac{\partial^2 T}{\partial z^2}\right)-\frac{1}{(\rho c_p)_{nf}}\frac{\partial q_r}{\partial z}+\frac{\mu_{nf}}{(\rho c_p)_{nf}}\left[\left(\frac{\partial u}{\partial z}\right)^2+\left(\frac{\partial v}{\partial z}\right)^2\right]$$

$$+\frac{\sigma_{nf}B_0^2}{(\rho c_p)_{nf}}\,[u^2+v^2]+\frac{Q_T}{(\rho c_p)_{nf}}(T_f-T_\infty). \quad (4)$$

The relevant boundary conditions for the present problem are;

$$u=u_w,\quad v=0,\quad w=0,-k_{nf}\frac{\partial T}{\partial z}=h_f\left(T_f-T\right)\ \ at\quad z=0,$$
$$u\to 0,\quad v\to 0,\quad T\to T_\infty\quad as\quad z\to\infty, \quad (5)$$

where u, v, and w are usual velocity components in x, y and z directions respectively, ω is constant angular velocity of the fluid, ρ_{nf} -density of the nanofluid, μ_{nf} -dynamic viscosity of nanofluid, α_{nf} -thermal diffusivity of nanofluid, C_p-specific heat at constant pressure, B_0-applied magnetic field strength, h_f -heat transfer coefficient, k_{nf}-thermal conductivity of nanofluid, T -temperature, $q_r=-\left(\frac{4\sigma^*}{3k^*}\right)\frac{\partial T^4}{\partial z}$ is the Rosseland radiative heat flux, σ^* -Stefan-Boltzman constant and k^* - mean absorption coefficient.

Brinkman [34] expressed the dynamic viscosity of nanofluid μ_{nf} as;

$$\mu_{nf}=\frac{\mu_f}{(1-\phi)^{2.5}}, \quad (6)$$

the effective density ρ_{nf} and effective heat capacity $(\rho c_p)_{nf}$ are expressed as [33];

$$\rho_{nf}=(1-\phi)\rho_f+\phi\rho_s, \quad (7)$$
$$(\rho c_p)_{nf}=(1-\phi)(\rho c_p)_f+\phi\left(\rho c_p\right)_s, \quad (8)$$

the Maxwell-Garnett model for effective thermal conductivity of nanofluid k_{nf} and k_f is thermal conductivity of base fluid given below,

$$\frac{k_{nf}}{k_f}=\frac{(k_s+2k_f)-2\phi(k_f-k_s)}{(k_s+2k_f)+\phi(k_f-k_s)}, \quad (9)$$

moreover, the electrical conductivity of nanofluid σ_{nf} is given in the book by Maxwell [35] as;

$$\frac{\sigma_{nf}}{\sigma_f}=1+\frac{3(\sigma_s-\sigma_f)\phi}{(\sigma_s+2\sigma_f)-(\sigma_s-\sigma_f)\phi}, \quad (10)$$

where $\left(\rho C_p\right)_s$-volumetric heat capacity of solid nanoparticles, $\left(\rho C_p\right)_f$, $\left(\rho C_p\right)_{nf}$-are volumetric heat capacities of base fluid and nanofluid respectively, ϕ -the particle volume fraction parameter of nanoparticles, ρ_f-density of base fluid, μ_f-dynamic viscosity of base fluid, k_s- thermal conductivity of solid nanoparticles, the subscripts s and f denotes to the solid and base fluid respectively and thermophysical properties of water and magnetite-Fe_3O_4 are given in Table 2.

Equations (1), (2), (3) and (4), subject to the boundary conditions (5) admit similarity solutions in terms of the similarity functions f, g, θ and the similarity variable η and are defined as;

$$u=axf'(\eta),\ v=axg(\eta),$$
$$w=-\sqrt{\nu_f a}f(\eta),\ \theta(\eta)=\frac{T-T_\infty}{T_f-T_\infty},\ \eta=\sqrt{\frac{a}{\nu_f}}z, \quad (11)$$

In view of the above quantities, the continuity Equation (2.1) is identically satisfied while Equations (2)-(5) become;

$$\frac{1}{(1-\phi)^{2.5}\left(1-\phi+\phi\frac{\rho_s}{\rho_f}\right)}f'''-f'^2+ff''+2\lambda g-\frac{\sigma_{nf}/\sigma_f}{\left(1-\phi+\phi\frac{\rho_s}{\rho_f}\right)}Mf'=0, \quad (12)$$

$$\frac{1}{(1-\phi)^{2.5}\left(1-\phi+\phi\frac{\rho_s}{\rho_f}\right)}g''+fg'-f'g-2\lambda f'-\frac{\sigma_{nf}/\sigma_f}{\left(1-\phi+\phi\frac{\rho_s}{\rho_f}\right)}Mg=0, \quad (13)$$

$$\frac{1}{\left(1-\phi+\phi\frac{(\rho c_p)_s}{(\rho c_p)_f}\right)}\left[\frac{1}{Pr}\left(\left(\frac{K_{nf}}{k_f}+R(1+(\theta_w-1)\theta)^3\right)\theta'\right)'\right]+f\theta'$$
$$+\frac{1}{\left(1-\phi+\phi\frac{(\rho c_p)_s}{(\rho c_p)_f}\right)}\left\{\frac{1}{(1-\phi)^{2.5}}Ec(f''^2+g'^2)+\frac{\sigma_{nf}}{\sigma_f}MEc(f'^2+g^2)\right\}$$
$$+\frac{Q_t\theta(\eta)}{\left(1-\phi+\phi\frac{(\rho c_p)_s}{(\rho c_p)_f}\right)}=0. \quad (14)$$

The corresponding boundary conditions become;

$$f'(0)=1,\ f(0)=0,\ g(0)=0\ \ \theta'(0)=Bi(\theta(0)-1)\quad \text{at}\quad \eta=0,$$
$$f'(\eta)\to 0,\ g(\eta)\to 0,\ \theta(\eta)\to 0 \text{ as}\quad \eta\longrightarrow\infty. \quad (15)$$

Non-dimensional quantities are magnetic parameter, ratio of rotation rate to the stretching rate parameter, Prandtl number, radiation parameter, heat soirce, Biot number, Eckert number, temperature ratio parameters are defined as;

$$M=\frac{\sigma_f {B_0}^2}{\rho_f a},\quad \lambda=\frac{\omega}{a},\quad Pr=\frac{(\mu c_p)_f}{k_f},\quad R=\frac{16\sigma^* T_\infty^3}{3k^* k_f},\quad Q_t=\frac{Q_T}{\rho_f c_{pf}}$$
$$Bi=\frac{h_f}{k_{nf}}\sqrt{\frac{\nu_f}{a}},\quad Ec=\frac{u_w^2}{c_{pf}(T_w-T_\infty)},\quad \theta_w=\frac{T_f}{T_\infty}. \quad (16)$$

The quantities of practical interest are the skin friction coefficients C_{fx}, C_{fy} and the local Nusselt number N_{ux} defined as follows;

$$C_{fx}=\frac{\tau_{wx}}{\rho_f u_w^2},$$
$$C_{fy}=\frac{\tau_{wy}}{\rho_f u_w^2},$$
$$Nu_x=\frac{x q_w}{k_f(T_w-T_\infty)}, \quad (17)$$

where $\tau_{wx}=\tau_{zx}|_{z=0}$ and $\tau_{wy}=\tau_{zy}|_{z=0}$ are the wall shear stresses and q_w is the wall heat flux given by,

$$\tau_{wx}=\mu_{nf}\frac{\partial u}{\partial z}|_{z=0},$$
$$\tau_{wy}=\mu_{nf}\frac{\partial v}{\partial z}|_{z=0},$$
$$q_w=-k_{nf}\frac{\partial T}{\partial z}|_{z=0}+q_r|_{z=0}. \quad (18)$$

Using equation (11) and (18) in equation (16) one obtains,

$$\sqrt{Re_x}\,C_{fx}=\frac{1}{(1-\phi)^{2.5}}f''(0),$$
$$\sqrt{Re_x}\,C_{fy}=\frac{1}{(1-\phi)^{2.5}}g'(0),$$
$$\frac{Nu_x}{\sqrt{Re_x}}=-\left(\frac{k_{nf}}{k_f}+R\theta_w^3\right)\theta'(0), \quad (19)$$

where $Re_x=\frac{u_w x}{\nu_f}$ is the local Reynolds number.

TABLE I THERMO-PHYSICAL PROPERTIES OF WATER BASED NANOFLUIDS.

	$\rho(kg/m^3)$	$c_p(J/kgK)$	$K(W/mk)$	$\sigma(\Omega m)^{-1}$
$Water$	997.1	4179	0.613	0.05
Fe_3O_4	5180	670	9.7	25000
Cu	8933	385	400	59.6
Al_2O_3	3970	765	40	16.7

TABLE II COMPARISON OF CURRENT RESULT WITH PREVIOUS STUDIES FOR SPECIAL CASES ($\phi = 0, M = 0$).

λ	Wang [22]		Nazar *et al.*,[23]		Present results	
	$f''(0)$	$g'(0)$	$f''(0)$	$g'(0)$	$f''(0)$	$g'(0)$
0	-1	0	-1	0	-1.00006	0
0.5	-1.1384	-0.5128	-1.1384	-0.5128	-1.13837	-0.51276
1.0	-1.3250	-0.8371	-1.3250	-0.8371	-1.32503	-0.83710
2.0	-1.6523	-1.2873	-1.6523	-1.2873	-1.65235	-1.28726

II. RESULTS AND DISCUSSION

The set of nonlinear ordinary differential equations is solved numerically using the Runge-Kutta-Fehlberg (RKF) method. In this numerical scheme, selecting a suitable finite value for η_max is crucial. Following standard boundary-layer theory, the asymptotic boundary conditions at $\eta \rightarrow \infty$ are approximated by a finite value η_∞. In the present computations, a step size of $\Delta\eta = 0.001$ is employed, and the convergence criterion is set to 10^(-6). To validate the accuracy of the numerical method, the computed values of f''(0) and g'(0) are compared with the benchmark results reported by Wang [22] and Nazar *et al.,*[23] for a special case. The comparison, summarized in Table II, shows excellent agreement.

Graphical illustrations of velocity and temperature profiles for various values of physical parameters—such as magnetic parameter (M), rotation parameter (λ), radiation parameter (R), Eckert number (Ec), heat source parameter (Q_t), and temperature ratio (θ_w)—are presented in Figs. 6-17 for Cu-, Al_2O_3-, and Fe_3O_4-water-based nanofluids. Furthermore, the effects of these parameters on the skin-friction coefficient and Nusselt number are analyzed and depicted in Figs. 2-5 for Cu- and Fe_3O_4-water-based nanofluids.

Equation 2 illustrates the variation of the skin-friction coefficient in the x-direction under the influence of λ and M. It is observed that increasing both parameters leads to a noticeable reduction in skin friction along the x-direction, indicating reduced surface shear stress due to enhanced magnetic damping and flow-stretching effects. Fig. 3 presents the skin-friction coefficient in the y-direction for varying λ and M. As λ increases, the skin friction in the y-direction decreases, reflecting reduced resistance in the transverse direction. In contrast, higher values of M result in an increase in skin friction along the y-direction, attributed to the intensified Lorentz force opposing the flow. Moreover, the velocity is found to be higher for Fe_3O_4-water-based nanofluid compared to Cu-based nanofluid, indicating superior flow characteristics and reduced resistance in Fe_3O_4 nanofluid due to its enhanced thermal and rheological properties.

Equation 4 presents the variation of the Nusselt number with λ and M. It is observed that the Nusselt number decreases with increasing λ and M, indicating a reduction in convective heat transfer at the surface. An increase in λ stretches the flow field, leading to a thinner thermal boundary layer but simultaneously weakens the thermal gradient at the wall. Similarly, a stronger magnetic field (higher M) induces a Lorentz force that suppresses fluid motion, lowering convective heat transfer rates and reducing the Nusselt number.

Equation 5 shows the combined effect of Ec and nanoparticle volume fraction (ϕ) on the Nusselt number. The results indicate that higher Ec and ϕ together lead to a notable enhancement in heat transfer, highlighting the effectiveness of nanoparticle-enriched fluids under high-energy dissipation conditions. Among the studied cases, Cu-water nanofluid exhibits the greatest improvement, followed by Fe_3O_4 nanofluid.

Equation 6 demonstrates the effect of Biot number (Bi) on the temperature profile. As Bi increases, fluid temperature also increases due to stronger convective heat exchange between the surface and the surrounding environment, leading to a thicker thermal boundary layer. Fig. 7 shows that increasing the heat source parameter raises the fluid temperature, as additional thermal energy is introduced through internal heat generation. Fig. 8 illustrates that higher Ec leads to an elevated temperature profile due to increased viscous dissipation effects.

Equation 9 and 10 depict the effect of M on the axial velocity f'(η) and transverse velocity g(η), respectively. Increasing M reduces the axial velocity but increases the transverse velocity due to the Lorentz force. Fig. 11 shows that the temperature and thermal boundary-layer thickness increase with higher M. Among the nanofluids, Cu-water nanofluid shows the highest enhancement, followed by Fe_3O_4 nanofluid. Figs. 12-14 present the effect of λ on velocity and temperature profiles. An increase in λ decreases the axial velocity but enhances the transverse velocity due to the Coriolis force, while also thickening the thermal boundary layer.

Equation 15 illustrates that higher radiation parameter R raises the temperature profile, while Equation 16 shows that increasing θ_w thickens the thermal boundary layer. A comparative analysis reveals that Cu-water nanofluid achieves the greatest heat-transfer enhancement, followed by Fe_3O_4 nanofluid. Finally, Equation. 17 shows that increasing ϕ raises the temperature due to enhanced thermal conductivity and diffusivity of the nanofluid, leading to more effective heat transfer.

III. CONCLUSION

This study presents a comparative evaluation of heat transfer performance between Cu and Fe_3O_4 water-based nanofluids under various physical effects. The results indicate that both the stretching ratio (λ) and the magnetic parameter (M) reduce convective heat transfer due to suppressed axial flow and weakened thermal gradients. However, the inclusion of nanoparticles significantly enhances heat transfer, with Cu-based nanofluids demonstrating the highest improvement owing to their superior thermal conductivity. Increasing the Eckert number (Ec) and nanoparticle volume fraction (ϕ) synergistically increases the Nusselt number, highlighting the combined effects of viscous dissipation and nanoparticle dispersion. Higher Biot number and heat source parameter values result in elevated temperatures and thicker thermal boundary layers, indicating improved surface-to-fluid heat exchange. Magnetic and Coriolis forces reshape the flow and thermal fields, indirectly influencing heat transfer. Radiation and temperature ratio parameters further intensify thermal profiles. Fe_3O_4 nanofluids exhibit better flow characteristics, while Cu nanofluids provide superior thermal efficiency. Overall, Cu-based nanofluids are optimal for heat-intensive applications, whereas Fe_3O_4 nanofluids offer balanced performance in thermally and flow-sensitive systems.

A. Acknowledgment: The authors are grateful to the reviewers and editors for their constructive suggestions.

B. Disclosure Statement: This research did not receive any specific grant from funding agencies in the public, commercial, or not-for-profit sectors.

C. Data Availability: The data supporting the findings of this study are available within the article.

D. Conflict of Interest: The authors declare that there is no conflict of interest regarding the publication of this paper.

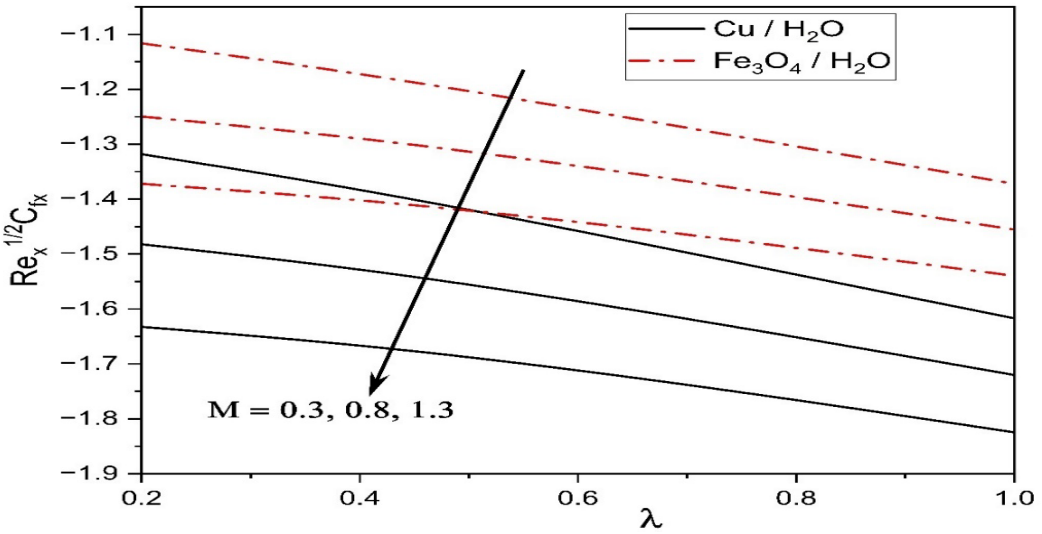

Fig.2 The effects of magnetic parameter v/s ratio of rotation rate to the stretching rate parameter on skin friction coefficient.

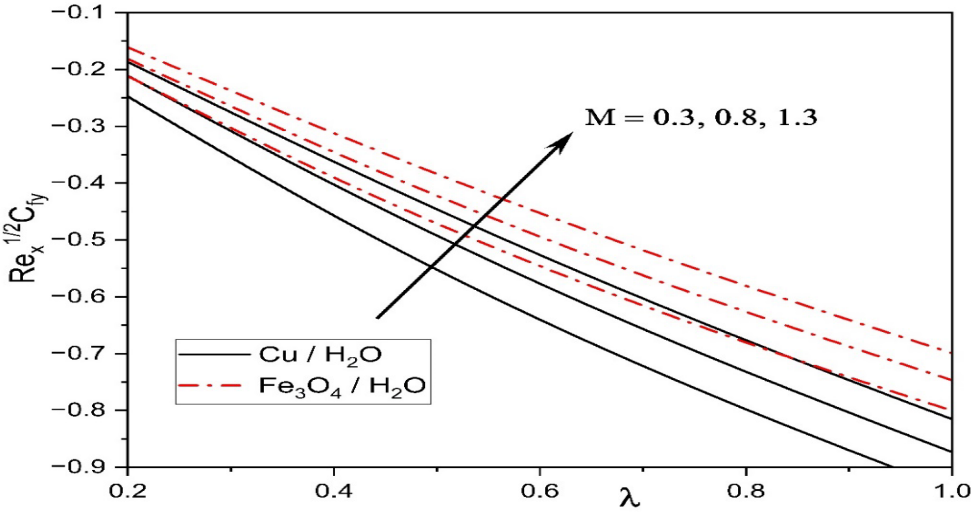

Fig.3 The effects of magnetic parameter v/s ratio of rotation rate to the stretching rate parameter on skin friction coefficient.

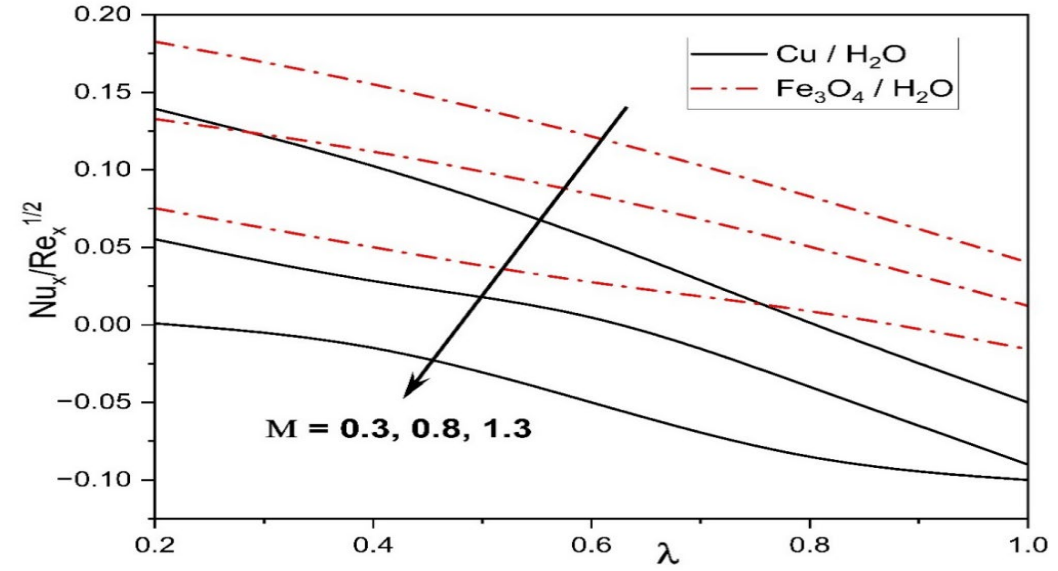

Fig.4 The effects of magnetic parameter v/s ratio of rotation rate to the stretching rate parameter on Nusselt number.

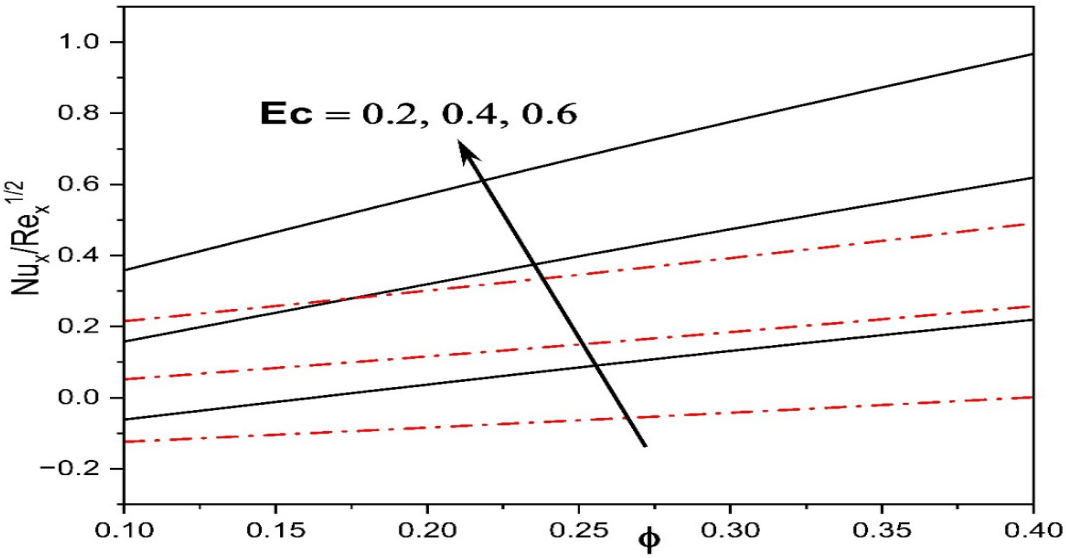

Fig.5 The effects of Eckert number v/s ϕ on Nusselt number.

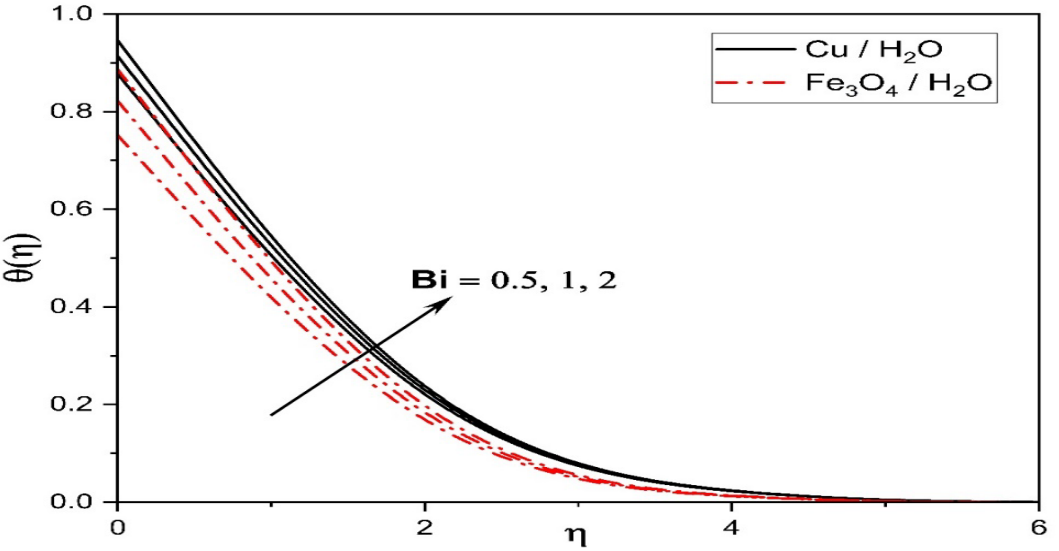

Fig.6 The effect of Biot number on temperature profile.

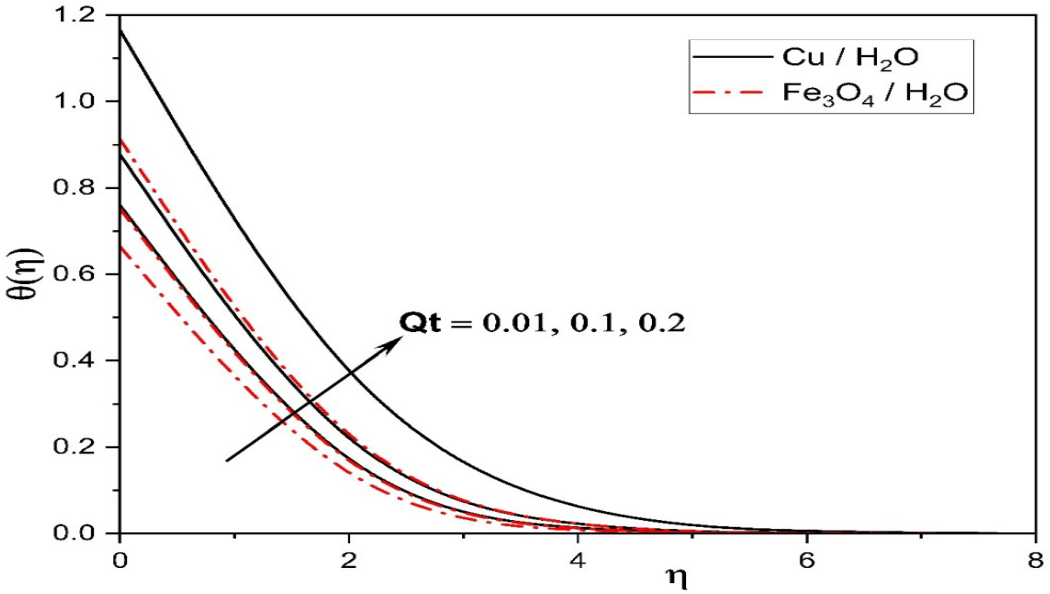

Fig.7 The effect of heat source parameter on temperature profile.

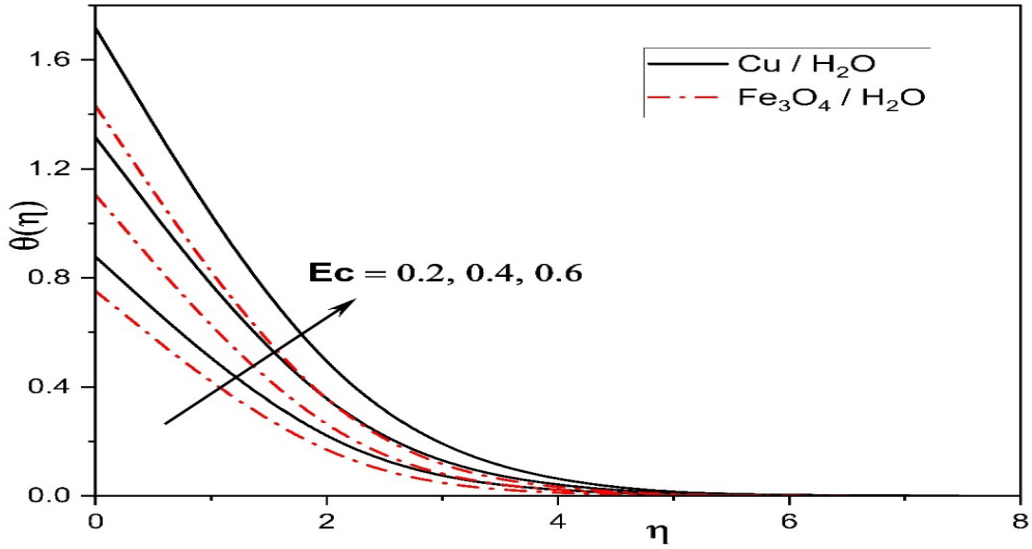

Fig.8 The effect of Eckert number on temperature profile.

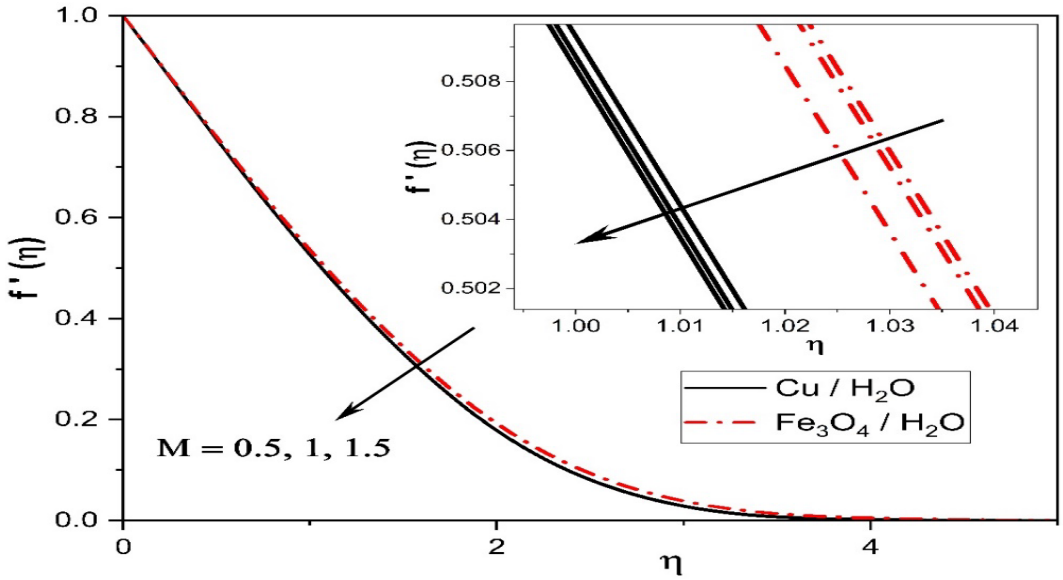

Fig.9 The effect of magnetic parameter on velocity profile.

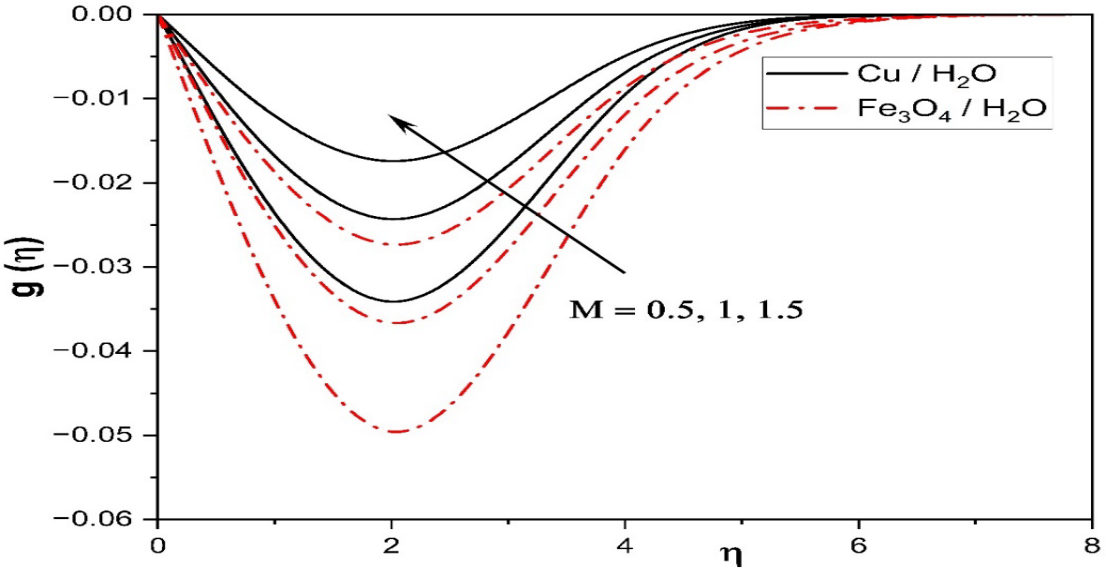

Fig. 10 The effect of magnetic parameter on velocity profile.

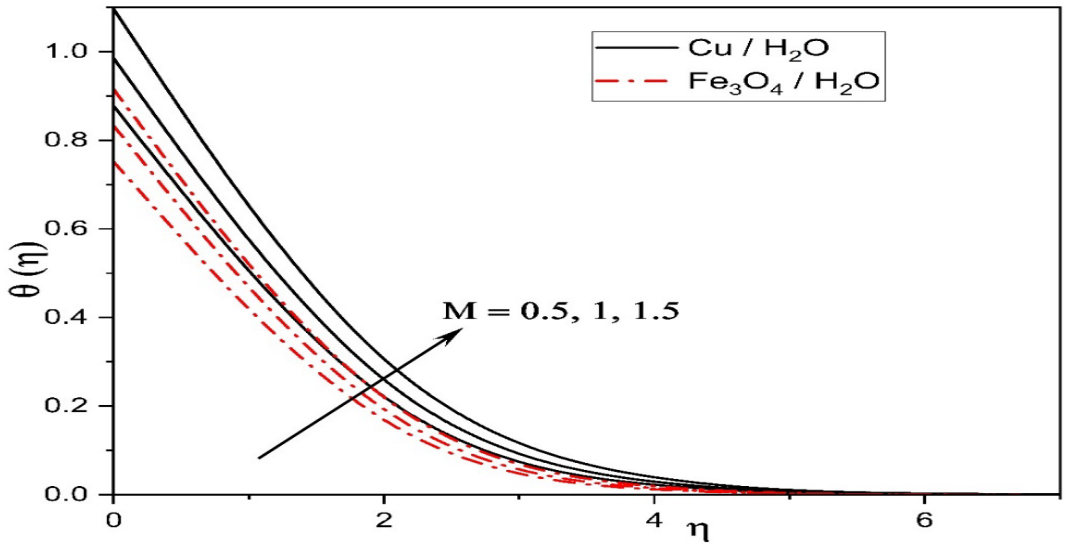

Fig.11 The effect of magnetic parameter on temperature profile.

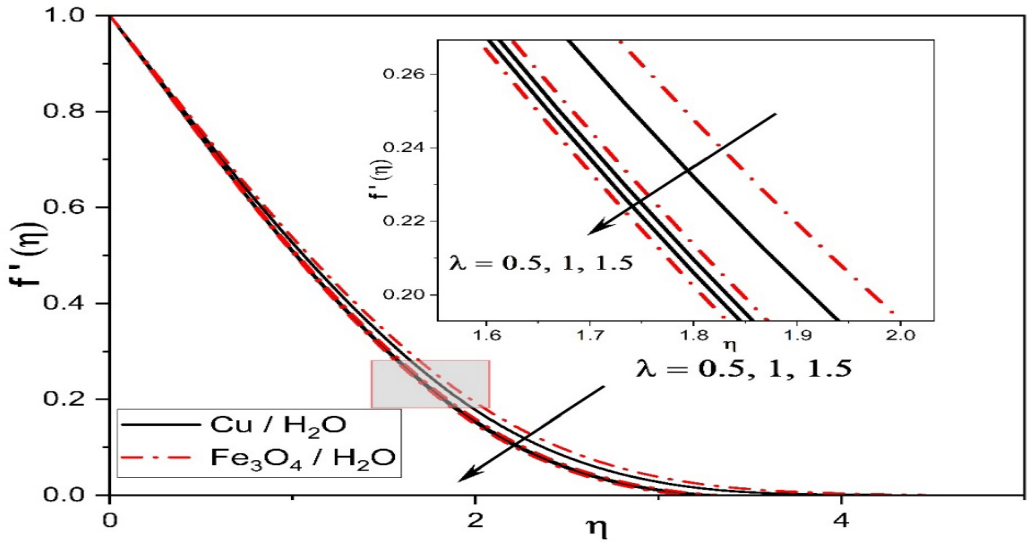

Fig.12 The effect of ratio of rotation rate to the stretching rate parameter on velocity profile.

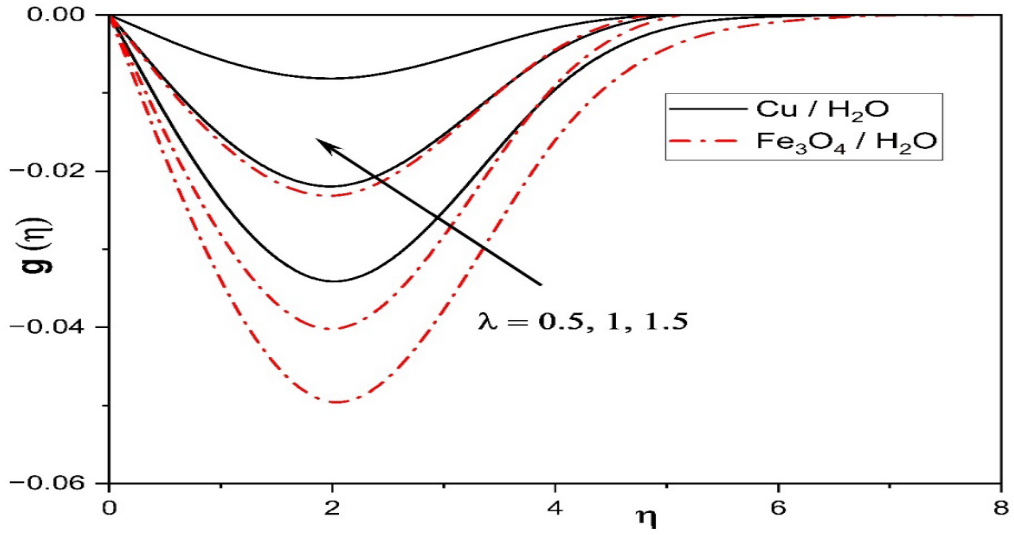

Fig.13 The effect of ratio of rotation rate to the stretching rate parameter on velocity profile

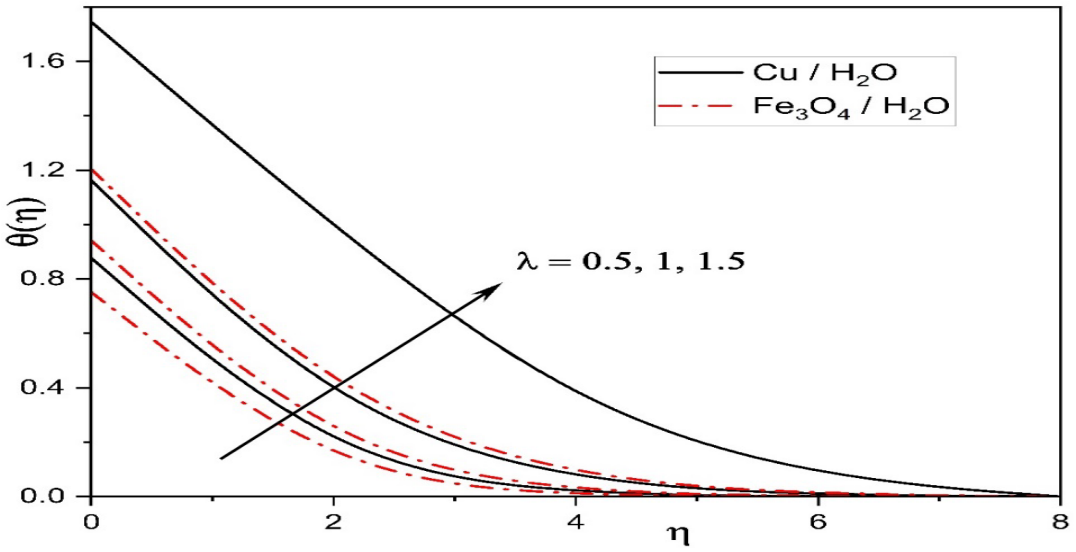

Fig.14 The effect of ratio of rotation rate to the stretching rate parameter on temperature profile.

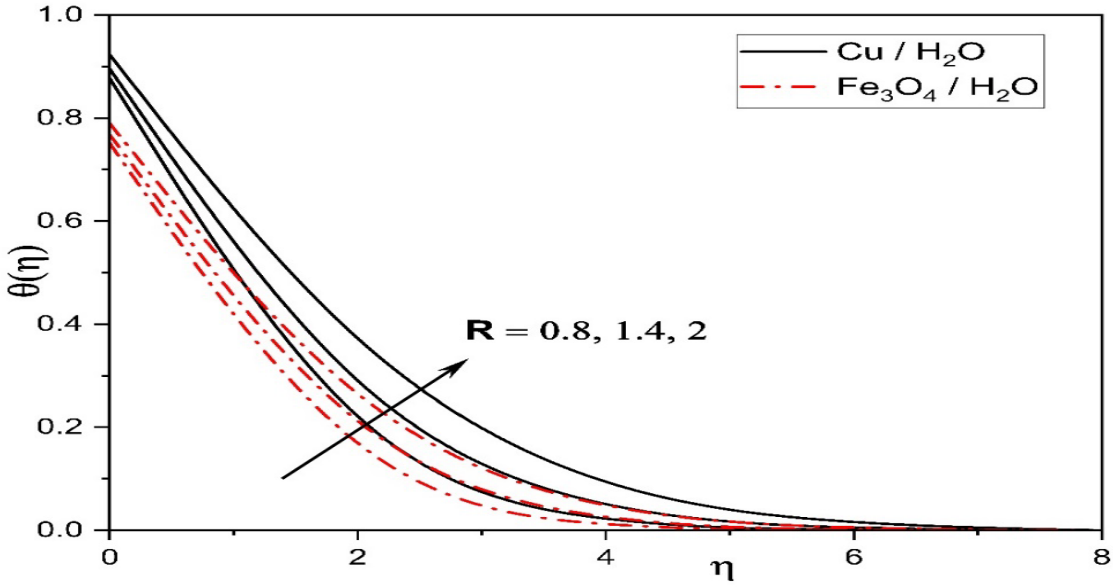

Fig.15 The effect of radiation parameter on temperature profile.

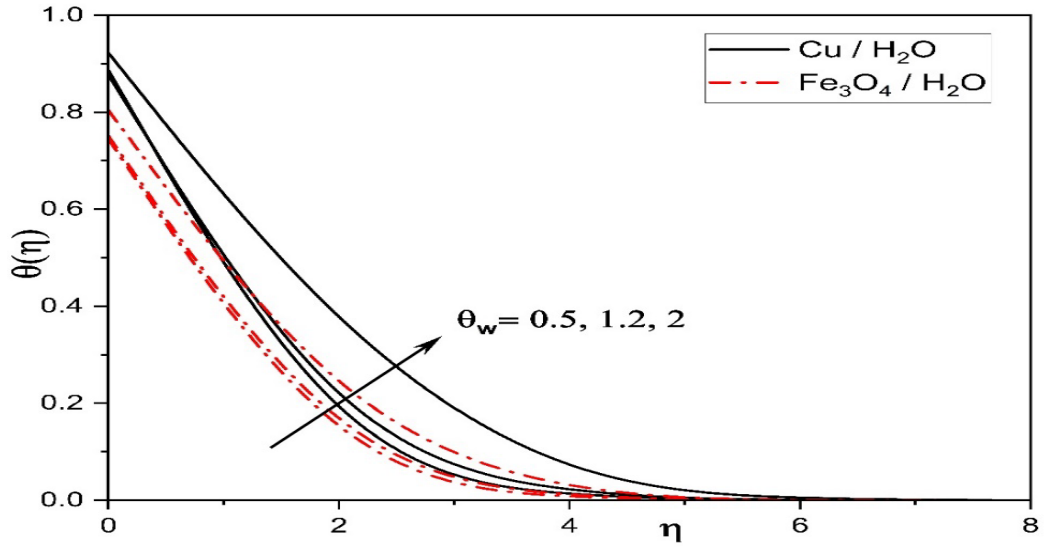

Fig.16 The effect of temperature ratio parameter on temperature profile.

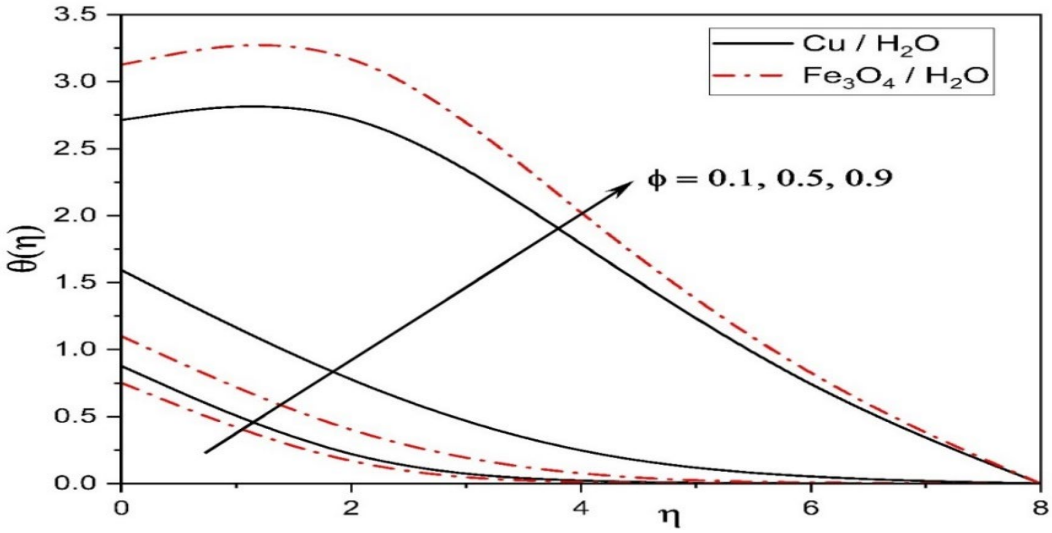

Fig.17 The effect of solid volume fraction parameter on temperature profile.

Declaration of Conflicting Interests
The authors declare no potential conflicts of interest with respect to the research, authorship, and/or publication of this article.

Funding
The authors received no financial support for the research, authorship, and/or publication of this article.

Use of Artificial Intelligence (AI)-Assisted Technology for Manuscript Preparation
The authors confirm that no AI-assisted technologies were used in the preparation or writing of the manuscript, and no images were altered using AI.

REFERENCES

[1] S. U. Choi and J. A. Eastman, "Enhancing thermal conductivity of fluids with nanoparticles," ANL/MSD/CP-84938; CONF-951135-29, Argonne National Lab., Argonne, IL, USA, 1995.

[2] L. Syam Sundar, K. V. Sharma, M. T. Naik, and M. K. Singh, "Empirical and theoretical correlations on viscosity of nanofluids: a review," *Renewable and Sustainable Energy Reviews*, vol. 25, pp. 670-686, 2013.

[3] M. Sajid *et al.,* "Journal of Thermal Analysis and Calorimetry," vol. 147, pp. 11259-11273, 2022.

[4] F. Mebarek-Oudina, "Powder Technology," vol. 424, p. 117567, 2023.

[5] J. Buongiorno, "Convective transport in nanofluids," *ASME J. Heat Transf.*, vol. 128, pp. 240-250, 2006.

[6] N. Muqaddass, F. Mabood, S. A. Shehzad, F. Sahar, and I. A. Badruddin, "Analysis of heat transportation in a convectively heated time-dependent $CuAl_2O_3$-H_2O hybrid nanofluid with varying thermal conductivity," *Proc. Inst. Mech. Eng., Part C: J. Mech. Eng. Sci.*, vol. 238, no. 6, pp. 2513-2520, 2024.

[7] A. Asadi, I. M. Alarifi, and L. K. Foong, "An experimental study on characterization, stability and dynamic viscosity of CuO-TiO_2/water hybrid nanofluid," *J. Mol. Liq.*, vol. 307, p. 112987, 2020.

[8] W. A. Khan and I. Pop, "Boundary-layer flow of a nanofluid past a stretching sheet," *Int. J. Heat Mass Transf.*, vol. 53, no. 11-12, pp. 2477-2483, 2010.

[9] M. Sheikholeslami and H. B. Rokni, "Nanofluid two-phase model analysis in existence of induced magnetic field," *Int. J. Heat Mass Transf.*, vol. 107, pp. 288-299, 2017.

[10] S. Nadeem, N. Abbas, and M. Y. Malik, "Inspection of hybrid based nanofluid flow over a curved surface," *Comput. Methods Programs Biomed.*, vol. 189, p. 105193, 2020.

[11] M. R. Krishnamurthy, B. J. Gireesha, R. S. R. Gorla, and B. C. Prasannakumara, "Suspended particle effect on slip flow and melting heat transfer of nanofluid over a stretching sheet embedded in a porous medium in the presence of nonlinear thermal radiation," *J. Nanofluids*, vol. 5, no. 4, pp. 502-510, 2016.

[12] K. U. Rehman, M. Y. Malik, O. D. Makinde, and A. A. Malik, "A comparative study of nanofluids flow yields by an inclined cylindrical

surface in a double stratified medium," *Eur. Phys. J. Plus*, vol. 132, no. 10, p. 427, 2017.

[13] D. Makinde, "Computational modelling of nanofluids flow over a convectively heated unsteady stretching sheet," *Curr. Nanoscience*, vol. 9, no. 5, pp. 673-678, 2013.

[14] N. S. Akbar, M. F. Hussain, M. Alghamdi, and T. Muhammad, "Thermal characteristics of magnetized hybrid Casson nanofluid flow in a converging-diverging channel with radiative heat transfer: A computational analysis," *Sci. Rep.*, vol. 13, no. 1, p. 21891, 2023.

[15] U. Khan, I. Waini, A. Zaib, A. Ishak, and I. Pop, "MHD mixed convection hybrid nanofluids flow over a permeable moving inclined flat plate in the presence of thermophoretic and radiative heat flux effects," *Mathematics*, vol. 10, no. 7, p. 1164, 2022.

[16] B. J. Gireesha and L. Anitha, "Convective flow of couple stress ternary nanoliquid flow through a permeable microchannel: irreversibility analysis," *Int. J. Model. Simul.*, pp. 1-18, 2024.

[17] J. K. Madhukesh, G. K. Ramesh, H. N. Fatima, G. S. Roopa, and S. A. Shehzad, "Influence of pollutant dispersion on nanofluid flowing across a stretched disc-cone device," *J. Mol. Liq.*, vol. 411, p. 125710, 2024.

[18] W. Cheng, M. Safeer, U. Farooq, S. Munir, J. Cui, and C. S. K. Raju, "Nonsimilar forced convection simulations of water-copper nanofluid flow through a porous medium in the presence of thermal radiations, heat generation and viscous dissipation," *Waves Random Complex Media*, vol. 35, no. 1, pp. 511-526, 2025.

[19] M. Sheikholeslami and S. A. Shehzad, "Magnetohydrodynamic nanofluid convection in a porous enclosure considering heat flux boundary condition," *Int. J. Heat Mass Transf.*, vol. 106, pp. 1261-1269, 2017.

[20] D. K. Jyoti, V. Nagaradhika, P. B. S. Kumar, and A. J. Chamkha, "Nonlinear convection and radiative heat transfer in kerosene-alumina nanofluid flow between two parallel plates with variable viscosity," *J. Nanofluids*, vol. 13, no. 5, pp. 1055-1062, 2024.

[21] T. V. Kármán, "Über laminar and turbulent Reibung," *ZAMM J. Appl. Math. Mech.*, vol. 1, no. 4, pp. 233-252, 1921.

[22] C. Y. Wang, "Stretching a surface in a rotating fluid," *ZAMP*, vol. 39, no. 2, pp. 177-185, 1988.

[23] R. Nazar, N. Amin, and I. Pop, "Unsteady boundary layer flow due to a stretching surface in a rotating fluid," *Mech. Res. Commun.*, vol. 31, no. 1, pp. 121-128, 2004.

[24] O. D. Makinde, O. A. Bég, and H. S. Takhar, "Magnetohydrodynamic viscous flow in a rotating porous medium cylindrical annulus with an applied radial magnetic field," *Int. J. Appl. Math. Mech.*, vol. 5, no. 6, pp. 68-81, 2009.

[25] M. Mustafa, A. Mushtaq, T. Hayat, and A. Alsaedi, "Rotating flow of magnetite-water nanofluid over a stretching surface inspired by non-linear thermal radiation," *PLoS One*, vol. 11, no. 2, p. e0149304, 2016.

[26] M. Archana, B. J. Gireesha, B. C. Prasannakumara, and R. S. R. Gorla, "Influence of nonlinear thermal radiation on rotating flow of Casson nanofluid," *Nonlinear Eng.*, 2017.

[27] P. B. S. Kumar, B. J. Gireesha, B. Mahanthesh, and R. S. R. Gorla, "Radiative nonlinear 3D flow of ferrofluid with Joule heating, convective condition and Coriolis force," *Thermal Sci. Eng. Prog.*, vol. 3, pp. 88-94, 2017.

[28] T. Hayat, Z. Abbas, I. Pop, and S. Asghar, "Effects of radiation and magnetic field on the mixed convection stagnation-point flow over a vertical stretching sheet in a porous medium," *Int. J. Heat Mass Transf.*, vol. 53, no. 1-3, pp. 466-474, 2010.

[29] T. G. Motsumi and O. D. Makinde, "Effects of thermal radiation and viscous dissipation on boundary layer flow of nanofluids over a permeable moving flat plate," *Phys. Scr.*, vol. 86, no. 4, p. 045003, 2012.

[30] M. Sheikholeslami, T. Hayat, and A. Alsaedi, "MHD free convection of Al_2O_3-water nanofluid considering thermal radiation: a numerical study," *Int. J. Heat Mass Transf.*, vol. 96, pp. 513-524, 2016.

[31] S. Jana Reddy, P. Valsamy, and D. S. Reddy, "Thermal radiation impact on nanofluid boundary layer flow towards a moving plate in presence of magnetic field using numerical solutions," *J. Nanofluids*, vol. 13, no. 1, pp. 199-206, 2024.

[32] H. Waqas, U. Farooq, D. Liu, M. Abid, M. Imran, and T. Muhammad, "Heat transfer analysis of hybrid nanofluid flow with thermal radiation through a stretching sheet: A comparative study," *Int. Commun. Heat Mass Transf.*, vol. 138, p. 106303, 2022.

[33] R. K. Tiwari and M. K. Das, "Heat transfer augmentation in a two-sided lid-driven differentially heated square cavity utilizing nanofluids," *Int. J. Heat Mass Transf.*, vol. 50, pp. 2002-2018, 2007.

[34] H. C. Brinkman, "The viscosity of concentrated suspensions and solutions," *J. Chem. Phys.*, vol. 20, pp. 571-581, 1952.

[35] J. C. Maxwell, *A Treatise on Electricity and Magnetism*, 2nd ed., Cambridge, UK: Oxford Univ. Press, 1904, pp. 435-441.